



Article

Rheological properties of magnesium bentonite and sepiolite suspensions after dynamic ageing at high temperatures

Georgios E. Christidis¹ , Nikolaos Athanasakis²  and Dimitrios Marinakis³ 

¹Technical University of Crete, School of Mineral Resources Engineering, 73100 Chania, Greece; ²KU Leuven, Department of Material Science, Arenberg, Belgium and ³University of Western Macedonia, Department of Mineral Resources Engineering, Kozani, Greece

Abstract

The rheological properties of three Na-activated, trioctahedral Mg-bentonites (hectorite clay from the CMS Source Clay Project repository, saponite clay from Spain and stevensite clay from Rhassoul, Morocco) and a sepiolite clay from Greece were examined after dynamic ageing at temperatures up to 230°C. The 5% w/v suspensions were prepared by dispersing the clay mineral samples in distilled water. The suspensions underwent dynamic, thermal ageing for 16 h before determination of the viscosity, filtration loss, filter cake thickness and pH and the concentration of dissolved Na⁺ and Mg²⁺. Thermal ageing contributed to the dispersion of clay particles, with a direct effect on plastic and apparent viscosity, introducing pseudoplastic behaviour. With the exception of the stevensite clay at 230°C that displayed limited dissolution at 230°C and partial conversion to kerolite, the clays were stable at high temperatures. The Na-activation of all clays except for stevensite was not adversely affected by thermal ageing. Thermal ageing of stevensite at 230°C facilitated Na exchange and yielded suspension with high viscosity and low filtrate loss. Only the suspensions of hectorite and those of stevensite aged at 230°C met with American Petroleum Institute specifications. The thermal behaviour and rheological properties of the clays might be interpreted according to the intrinsic properties of the clay minerals, such as layer charge and charge distribution.

Keywords: Alkali activation; drilling fluids; hectorite; Mg-bentonite; rheological properties; saponite; sepiolite; stevensite; thermal ageing
(Received 10 December 2023; revised 6 April 2024; accepted 7 April 2024; Accepted Manuscript online: 30 April 2024)

Drilling fluids are an integral part of the oil and gas extraction process because they seal and support the walls of the well from the water of the surrounding formations by increasing the hydrostatic pressure inside the well (McKee & Geehan, 1989). In addition, they serve as coolants and lubricants for the drilling bits whilst transporting the fragmented rock to the surface, and they protect the drilling equipment from corrosion (McDonald *et al.*, 2007; Temraz & Hassanien, 2016).

A drilling fluid consists of a fluid phase, in which one or several solid phases are dispersed. The fluid phase can be aqueous (water-based muds; WBMs), oily (oil-based muds; OBMs), gaseous or emulsions (Vryzas & Kelessidis, 2017; Zhang *et al.*, 2020). The solid phases consist of a series of different materials that regulate the rheological properties of the suspension, the most important of which are clay mineral nanoparticles (mainly Na-smectite in the form of Na-bentonite, sepiolite and palygorskite; Güven, 1992; Neaman & Singer, 2000a,b; Christidis, 2011; Zhang *et al.*, 2020). The main clay material used in drillings is Na-bentonite (Gautam *et al.*, 2018). Smectites, the main mineral of bentonites, are characterized by flaky crystals, with a particle

size of <0.5 µm, whilst carrying a negative electrical charge located in octahedral and/or tetrahedral sites (Odom, 1984; Meunier, 2005). By contrast, palygorskite and sepiolite form fibrous crystals of <2 µm in size, which are not characterized by significant layer charge (Meunier, 2005). These properties contribute to the formation of stable, non-Newtonian, viscous fluids (Lagaly, 1989; Christidis & Scott, 1996; Christidis, 1998; Neaman & Singer, 2000a,b). Additives, namely polymers (xanthan gum, polyanionic cellulose, etc.; Bavoh *et al.*, 2022), weighting agents (barite, hematite, etc.; Bageri *et al.*, 2021) and nanoparticles (including magnetite, sepiolite, etc.; Gerogiorgis *et al.*, 2015; Al-Malki *et al.*, 2016), are incorporated into the suspensions, improving their performance.

To date, research studies in this area have focused on understanding the rheological properties of Na-bentonites for application in the drilling industry. These studies involve almost exclusively dioctahedral smectites with octahedral charge, mainly montmorillonite (Brandenburg & Lagaly, 1988; Christidis & Scott, 1996; Christidis, 1998; Christidis *et al.*, 2006; Kelessidis *et al.*, 2007b; Kelessidis & Maglione, 2008; Vryzas & Kelessidis, 2017; Vryzas *et al.*, 2017) and mixtures of palygorskite or sepiolite with dioctahedral smectite (Chemeda *et al.*, 2014; Al-Malki *et al.*, 2016). In addition, substantial work has been carried out in the last two decades relevant to the rheological behaviour of water-based and oil-based sepiolite drilling fluids (for a review,

Corresponding author: Georgios E. Christidis; Email: gchristidis@tuc.gr
Cite this article: Christidis GE, Athanasakis N, Marinakis D. Rheological properties of magnesium bentonite and sepiolite suspensions after dynamic ageing at high temperatures. *Clay Minerals*. <https://doi.org/10.1180/clm.2024.11>

© The Author(s), 2024. Published by Cambridge University Press on behalf of The Mineralogical Society of the United Kingdom and Ireland. This is an Open Access article, distributed under the terms of the Creative Commons Attribution-NonCommercial-NoDerivatives licence (<http://creativecommons.org/licenses/by-nc-nd/4.0>), which permits non-commercial re-use, distribution, and reproduction in any medium, provided that no alterations are made and the original article is properly cited. The written permission of Cambridge University Press must be obtained prior to any commercial use and/or adaptation of the article.

see Zhang *et al.*, 2020). Sepiolite enhances the performance of drilling fluids functioning as thixotropic and thickening agents (Alvarez, 1984) and augments their gel strength, plastic viscosity (PV) and yield point (YP; Abdo *et al.*, 2016).

Most studies on the rheological properties of water-based and oil-based drilling fluids, prepared with various types of clays, have been performed at room temperature and after ageing at room temperature (Brandenburg & Lagaly, 1988; Christidis & Scott, 1996; Christidis, 1998; Neaman & Singer, 2000a; Christidis *et al.*, 2006; Kelessidis *et al.*, 2007b; İşçi & Turutoğlu, 2011; Chemedi *et al.*, 2014; Al-Malki *et al.*, 2016; Zhuang *et al.*, 2018; Echt & Plank, 2019). Studies on the effects of temperature on the rheological properties of clay suspensions at high temperatures and pressures are less common and have focused mainly on montmorillonite suspensions (Hiller, 1963; Alderman *et al.*, 1988; Briscoe *et al.*, 1994; Santoyo *et al.*, 2001; Kelessidis *et al.*, 2007a,c; Mohammed, 2017; Vryzas *et al.*, 2017), especially Wyoming montmorillonite.

By contrast, studies on the rheological properties of clays with trioctahedral clay minerals, both bentonites and sepiolite, used as drilling fluid additives both at ambient conditions and at elevated temperatures and pressures are limited. Güven *et al.* (1988) studied the rheological properties of clays rich in saponite, sepiolite and Wyoming montmorillonite at a temperature range of 149–316°C and reported high stability and viscosity of the saponite-based fluid when interacting with electrolytes. The rheological behaviour of a series of dioctahedral smectites and hectorite at room temperature was reported by Christidis *et al.* (2006), and Xiong *et al.* (2019a,b) observed excellent dispersibility and stability of laponite, the artificial counterpart of hectorite, at high temperatures, making it a potential candidate for drilling in high-temperature environments. Laponite is not pure hectorite but a mixture of hectorite and stevensite with ~25% non-swelling disordered talc (kerolite) layers (Christidis *et al.*, 2018). Laponite was also tested as additive in bentonite suspensions and was reported to be successful at temperatures as high as 150°C (Li *et al.*, 2022). Mixtures of clays containing montmorillonite/saponite or sepiolite/saponite retain and even enhance the advantages of these trioctahedral clay minerals in various applications, including drilling fluids (Güven *et al.*, 1987, 1992; Miles, 2011).

Trioctahedral smectites, namely hectorite, stevensite and saponite (the main constituents of Mg-bentonites), are 2:1 clay minerals, with their octahedral sites occupied by Mg²⁺ cations (Brigatti *et al.*, 2013). Partial substitution of Li⁺ for Mg²⁺ yields the octahedral sheet of hectorite and introduces a negative layer charge (Meunier, 2005). The layer charge of stevensite originates from a small number of vacancies in the octahedral sheet (Brindley, 1984; Christidis & Mitsis, 2006). In the case of saponite, Si⁴⁺ cations are substituted by Al³⁺ cations in the tetrahedral sheet. In contrast to other smectites, saponite may have a positive octahedral charge due to the replacement of the structural Mg²⁺ cations by Al³⁺ or Fe³⁺, which partially balances the negative tetrahedral charge (Christidis, 2011; Madejová *et al.*, 2017). Sepiolite is a trioctahedral clay mineral with a fibrous structure (Newman & Brown, 1987), its octahedral sheets being continuous in one dimension, forming a ribbon-like structure. The layout of sepiolite tetrahedral sheets consists of inverted tetrahedra in every two or three rows. The above characteristics result in the formation of channels with dimensions 4.0 Å × 9.5 Å (Brigatti *et al.*, 2013). In this contribution, new data are provided on the rheological properties of Mg-bentonites with saponite-, hectorite-, stevensite- and sepiolite-rich clay suspensions and on the ability

of these clays to form filter cakes both at ambient temperature and after ageing (hot rolling) at elevated temperatures up to 230°C. The study particularly examines the importance of the intrinsic characteristics of the clays to rheological behaviour at these temperatures. Temperatures in excess of 120°C are encountered in oil drillings below 3000 m in depth, as well as in geothermal drillings of high enthalpy at shallow depths. Therefore, this work will be useful for predicting the behaviour of drilling fluids made from trioctahedral phyllosilicates in high-temperature settings, especially considering that the published information on natural Mg-clays is very limited and that the application of synthetic Mg-clay minerals such as laponite is an expensive solution for drilling fluid applications.

Materials and methods

Materials

Four Mg-rich clays were used in this study: three Mg-bentonites and one sepiolite sample (Table 1). The bentonites include SHCa-1 from Hector, CA, USA (CMS Source Clay Project), a saponite-rich bentonite from Vicalvaro Basin, Madrid, Spain, and a stevensite-rich bentonite from Jbel Ghassoul, Morocco (Benhammou *et al.*, 2009), known as Rhassoul or Ghassoul clay, supplied by Dr K. El Ass. The sepiolite sample comes from the rims of magnesite veins in the ophiolite complex of Euboea Island, Greece, and it was collected by the lead author.

Characterization methods

The bulk mineralogy of the samples was determined using X-ray diffraction (XRD), with a Bruker D8 Advance diffractometer equipped with a LynxEye silicon strip detector, using Ni-filtered Cu-K α radiation (35 kV, 35 mA), 0.298° divergence and anti-scatter slits, a step size of 0.019°2 θ and counting time of 1 s per strip step (total time = 63.6 s per step), in the 2 θ range of 4–70°2 θ . Data were evaluated using EVA[®] software provided by Bruker. Quantitative analysis was performed with the BGMN computer code (Autoquan[®] software package version 2.8) on random powder samples, prepared by grinding with an agate pestle and mortar and mounted by careful side loading on Al-holders to avoid a preferred orientation.

Thermogravimetric and differential thermogravimetric (TG-DTG) analyses of the <2 μ m fractions of clay samples were performed with a Perkin Elmer TGA-6 Thermal Analyser at the Laboratory of Solid Fuels Beneficiation and Technology of the School of Mineral Resources Engineering, Technical University of Crete. The clay fractions were separated according to Stokes' law after dispersion of bulk samples in distilled water. Analyses were performed in an inert atmosphere (N₂) in the temperature range 40–900°C with a heating rate of 10°C min⁻¹.

The major elemental composition of the clay samples was determined using energy-dispersive X-ray fluorescence (ED-

Table 1. Sample notation and origins of clay mineral samples used in this study.

Sample	Origin
SHCa-1 hectorite	CMS Source Clay Project
Saponite	Spain
Stevensite	Morocco
Sepiolite	Greece

XRF) spectroscopy with a Bruker S2 Ranger ED-XRF spectrometer on fusion beads using an 1:1 mixture of Li-tetraborate and Li-metaborate as the flux. The Li contents of hectorite and stevensite were determined using flame atomic emission spectrometry (FAES) with a Perkin Elmer Analyst 100 FAES device. The SDC-1 standard was used as a Li-rich reference sample. Prior to Li analysis, the samples were dissolved with a mixture of HCl, HNO₃ and HF acid solutions. The loss on ignition (LOI) was calculated by heating the samples at 1000°C. The cation-exchange capacity (CEC) of the clays was determined after saturation with 1 M ammonium acetate with a Kjeldahl microsteam distillator and titration with 0.05 N H₂SO₄.

Rheological properties

Viscosity

The materials were used without any prior purification. They were dried at 105°C and ground to pass through a 75 µm sieve. The bentonite samples were rendered Na-homoionic *via* the addition of optimal amounts of Na₂CO₃ determined from free swelling tests (c.f. Christidis *et al.*, 2006). The suspensions were prepared according to the American Petroleum Institute (API) specifications (API 13A, 2010), except for the concentration of the suspension (5% instead of 6.42% w/v), by adding the ground clay and the optimal amount of Na₂CO₃ in distilled water. The suspensions were stirred for 20 min and then were aged for 16 h at various temperatures (see below). Therefore, the bentonites used for rheological tests were Na-saturated. Activation was not performed on the sepiolite samples. The properties determined were apparent viscosity (AV), PV, yield stress and 10 min gel strength. The rheological properties of the samples were determined with a Grace 3500a Couette-type viscometer on clay suspensions in distilled water.

Dynamic thermal ageing was performed by transferring the agitated suspensions in stainless steel autoclaves (FANN Instrument Company, Houston, TX, USA). Ageing was performed at room temperature (25°C), 100°C, 149°C, 176°C and 230°C. After completion of each thermal ageing cycle, the suspensions were cooled down and stirred for 5 min and their pH values were recorded. pH acts as a stabilization factor for suspensions. In general, alkaline conditions promote stabilization, as clay particles acquire negative overall charges and repel each other (Tombácz *et al.*, 1990; Tombácz & Szekeres, 2004). At acidic pH values, the protons are adsorbed by the active edges of the clay mineral particles, whereas their edge charges become initially neutral and then positive (isoelectric point; van Olphen, 1977). The optimum pH for common drilling fluids ranges between 9 and 10 (Gamal *et al.*, 2019). The rheological experiments after ageing at 100°C and 149°C were performed in duplicate to estimate the repeatability of the measurements.

The rheological data were analysed using *M3600* software and plotted on shear stress *vs* shear rate charts (rheograms). The obtained curves corresponded to the Power Law, Herschel & Bulkley and Bingham Plastic rheological models, and the curves were fitted to the experimental data using an optimization routine written in *MATLAB*. The Herschel & Bulkley model looks identical to the Power Law model, with the difference being the presence of a yield stress parameter in the former model (Cheremisinoff, 1986). As the rheograms showed the existence of yield stress, the τ_0 parameter was constrained to >0 in the Herschel & Bulkley model and all parameters were allowed to vary in the positive range.

Filtrate loss

The filtrate loss determination is a simulation of the fluid loss due to filtering of the drilling fluid through the surrounding drilling wall. A low-pressure-low-temperature (LPLT) filter press (FANN Instrument Company) was used for the experiments. CO₂ was used as the pressure medium, and this was set at 6.9 atm (~100 psi). The API specifications set the limit of fluid loss for WBMs at 15 mL for a 30 min test run (API 13A, 2010). The filtrate loss volume collected during the first 7.5 min at 6.9 atm was not taken into account (API 13A, 2010). The expelled leachates were stored for further chemical analysis *via* flame absorption atomic spectrometry (FAAS) for their Na and Mg contents. The solids of those samples aged at 230°C were dried at 70°C and subsequently examined by XRD to trace possible mineralogical changes during thermal ageing using the same experimental setup described for the original materials.

Filter cake thickness

The thickness of the filter cake was measured with a calliper on the filter paper. In normal drilling operations, the cake also includes aggregated clay particles and other particles (i.e. cuttings, weighting agents, etc.) of different sizes, which reduce the permeability of the cake (Kelessidis *et al.*, 2006; van Oort *et al.*, 2016). In such cakes, the migration of the finer clay particles into the remainder of the pores and the saturation of the latter with the drilling fluid lead to even better sealing performance.

Results

Mineralogy of the trioctahedral clays

The bulk mineralogical composition of the Mg-clays is listed in Table 2. The samples have variable clay mineral contents. SHCa-1 consists mainly of hectorite and calcite, with minor quartz, dolomite and plagioclase and trace analcime. The stevensite clay consists almost exclusively of smectite (97.1%), with traces of dolomite and K-feldspar. The Spanish saponite sample consists mainly of smectite, with minor illite, quartz, K-feldspar and plagioclase. Finally, the sepiolite sample consists almost exclusively of sepiolite (97.5 wt.%), with minor brucite and trace dolomite. All clay minerals display 060 diffraction at 1.525–1.528 Å, confirming the trioctahedral nature of the smectites and the sepiolite.

After thermal ageing at 230°C, the Mg-clays displayed minor changes. The main modifications included the almost total dissolution of dolomite in hectorite, stevensite and sepiolite (Fig. 1a,b). In principle, the Mg-clay minerals were not affected by thermal

Table 2. Mineralogical composition of the clays (wt.%).

	SHCa-1	Stevensite	Saponite	Sepiolite
Smectite	48.5	97.1	85.4	n.d.
Sepiolite	n.d.	n.d.	n.d.	97.5
Quartz	2.4	n.d.	1.2	n.d.
K-feldspar	n.d.	2.0	3.7	n.d.
Albite	2.5	n.d.	4.4	n.d.
Analcime	0.5	n.d.	n.d.	n.d.
Dolomite	2.3	0.9	n.d.	0.5
Brucite (%)	n.d.	n.d.	n.d.	2.1
Illite (%)	n.d.	n.d.	5.3	n.d.
Calcite (%)	44.0	n.d.	n.d.	n.d.

n.d. = not detected.

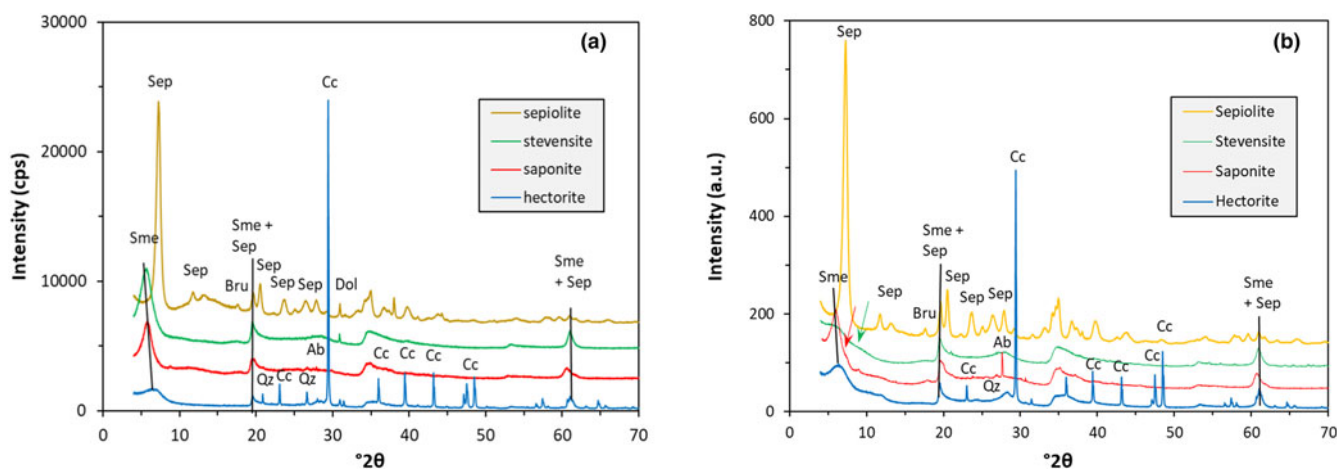


Figure 1. XRD traces of the trioctahedral clays. (a) Original materials and (b) materials after thermal ageing at 230°C. The green arrow indicates a ~ 10.5 Å phase in stevensite and the red arrow indicates a 12.7 Å component in saponite. See text for discussion. Ab = albite; Bru = brucite; Cc = calcite; cps = counts per second; Dol = dolomite; Qz = quartz; Sep = sepiolite; Sme = smectite.

ageing, with the exception of stevensite, in which the 001 diffraction maximum was split into two components: one at ~ 13 – 14 Å and a minor one at 10 – 10.5 Å. In addition, the Na-exchange was not complete, as is indicated by the location of the 001 diffraction maximum, which is centred at 13 – 14 Å. Saponite displayed a second 001 component in the form of a shoulder centred at ~ 12.8 Å, indicative of partial Na-exchange during ageing. The impact of Na-exchange on rheological behaviour after thermal ageing is addressed in the ‘Discussion’ section.

CEC determination

The CEC of clay minerals is a result of the permanent electric charge due to isomorphous substitutions in the tetrahedral and octahedral sheets (Johnston & Tombácz, 2002). Additionally, the exposed active edges of the crystals introduce a pH-dependent electric charge, which contributes up to 5% to the overall charge and consequently increases CEC (Grim, 1962). Smectites acquire CEC values of between 80 and 150 $\text{cmol}_c \text{ kg}^{-1}$ of dry clay (Bergaya & Vayer, 1997; Grim, 1968). The stevensite clay is the only bentonite sample that has a CEC value within the accepted CEC range. Hectorite contains only 48.5% smectite, which explains its reduced CEC. Contrary to expectations, saponite has the lowest CEC, even though it contains 85.4% smectite. Sepiolites present lower CEC values than bentonites, as expected.

Chemical composition of the trioctahedral clays

The chemical composition of the studied clays is listed in Table 3 and is in accordance with the majority of trioctahedral phyllosilicates. MgO is the most abundant constituent after SiO₂ in all of the samples, except for hectorite. Hectorite has a high CaO content and LOI and lower SiO₂ and MgO contents compared to the other samples due to the presence of abundant calcite and the lower Mg-smectite content. Minor Li₂O is present in hectorite and trace Li₂O (380 ppm) is present in stevensite. The presence of Li is associated with octahedral substitutions of Li for Mg, and its presence in stevensite indicates the existence of trace hectorite layers in the sample. Saponite is richer in Al₂O₃ and K₂O than its counterparts, which is in accordance with the tetrahedral

Al in the mineral and the presence of illite and plagioclase impurities. Saponite also has a greater Fe₂O₃ content, linked to octahedral substitutions. Finally, sepiolite contains small amounts of NiO, which is in accordance with the origin of the material in ophiolite rocks.

TG-DTG analysis

The TG-DTG tests provide information regarding the dehydration and dehydroxylation temperatures of the clay minerals (Sainz-Diaz *et al.*, 2001). Trioctahedral smectites dehydroxylate at higher temperatures ($\sim 800^\circ\text{C}$) compared to their dioctahedral counterparts ($< 700^\circ\text{C}$; Wolters & Emmerich, 2007). The TG and DTG curves of the $< 2 \mu\text{m}$ clay fractions are shown in Fig. 2. All samples show a main weight loss event due to removal of adsorbed water at between 100°C and 150°C (Fig. 2a,b). Stevensite expels crystalline water in four distinct stages: at $\sim 320^\circ\text{C}$, 400 – 500°C , 600°C and 800°C (Fig. 2b). The main dehydroxylation event is observed at 800°C . Hectorite also displays three water loss events associated with dehydroxylation, at $\sim 660^\circ\text{C}$, $\sim 760^\circ\text{C}$ and $\sim 835^\circ\text{C}$, in accordance with Guggenheim & Koster van Groos (2001). The latter thermal event might receive contribution from trace fine-grained calcite, which

Table 3. Chemical composition and CEC of the studied clays.

Component (wt.%)	Hectorite	Saponite	Stevensite	Sepiolite
SiO ₂	34.43	48.63	48.83	53.16
TiO ₂	0.03	0.28	0.13	bdl
Al ₂ O ₃	1.21	8.51	2.34	0.63
Fe ₂ O ₃	0.33	3.30	1.05	0.12
MnO	0.01	0.10	0.01	bdl
MgO	15.42	24.52	27.48	26.55
CaO	23.08	1.30	1.41	0.96
Na ₂ O	1.93	1.03	1.32	1.19
K ₂ O	0.06	1.07	0.52	bdl
Li ₂ O	0.62	bdl	0.04	bdl
P ₂ O ₅	0.54	0.02	0.20	bdl
NiO	bdl	bdl	bdl	0.34
LOI	22.22	10.90	15.91	17.18
Total	99.88	99.65	99.25	100.12
CEC ($\text{cmol}_c \text{ kg}^{-1}$)	51.5	86.2	48.6	33

bdl = below detection limit.

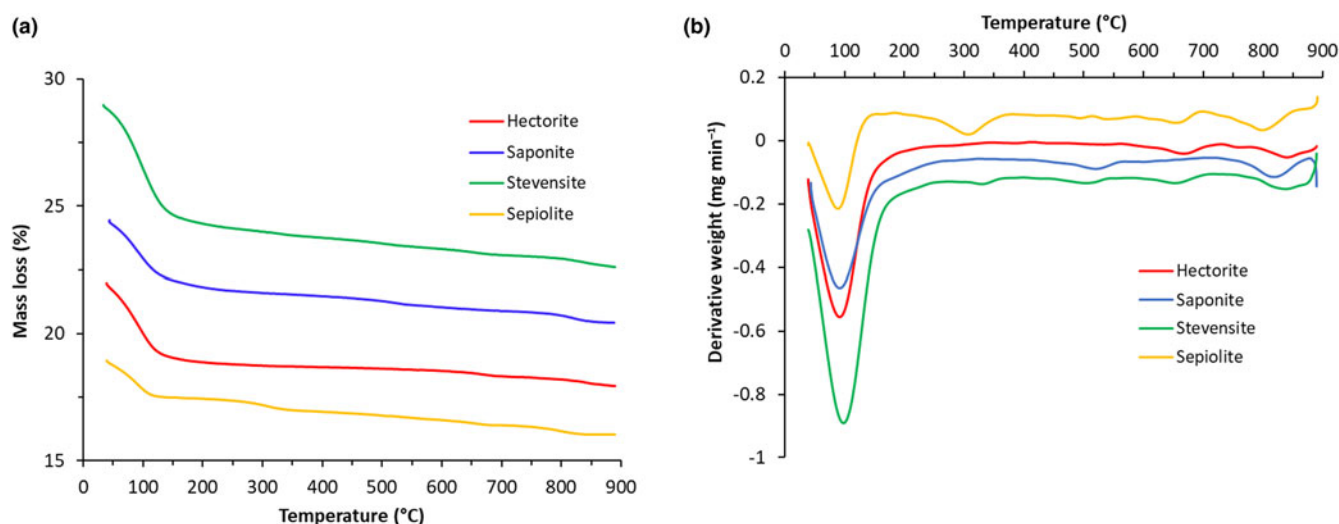


Figure 2. Thermal analysis of the studied clays. (a) TG curves; (b) DTG curves.

might also participate in the clay fraction. Considering that the weight loss of hectorite at $\sim 835^\circ\text{C}$, due to decomposition of calcite, is $\sim 0.20\%$, it follows that the calcite content in the clay fraction would be $\sim 0.45\%$. The saponite sample shows two endothermic events: a minor one at 500°C and a major one at $>800^\circ\text{C}$ (Fig. 2b). The event at 500°C is attributed to the presence – in minor concentration – of illite (Table 2), and possibly to minor stevensite layers that might be present in the sample. The sepiolite sample displays five endothermic events in addition to a low-temperature one (at $\sim 100^\circ\text{C}$), namely at $\sim 310^\circ\text{C}$, $\sim 490^\circ\text{C}$ and 550°C (doublet) and at 650°C and 800°C . The event at 490°C is associated with the dehydroxylation of minor brucite, and that at 650°C is associated with minor dolomite (Fig. 1 & Table 2). Finally, the events at 310°C , 550°C and 800°C are due to gradual dehydroxylation of sepiolite, with the event at 800°C receiving contribution from decarbonation of the CaCO_3 component of dolomite (Fig. 1 & Table 2). Thermal analysis results show that the maximum ageing temperature of the fluids is considerably lower than the temperatures of weight loss due to dehydroxylation of all of the trioctahedral smectites and sepiolite. Therefore, the thermal ageing is not expected to have caused dehydroxylation of the trioctahedral clay minerals, and any changes in the rheological properties of the suspensions at high temperatures, especially the ones at 230°C , are not related to structural changes to the clay minerals.

Rheological properties

Rheograms, rheological models and representative rheological parameters

Previous work has shown that bentonite-based suspensions display remarkable rheological performance up to 120°C (250°F), but at higher temperatures the addition of rheological additives, namely lignite and xanthan gum, has been recommended (Kelessidis *et al.*, 2006).

The rheograms of the different suspensions are shown in Fig. 3, the evolution of viscosity with ageing temperature is shown in Figure 4 and the main rheological parameters are summarized in Table 4. Hectorite suspensions became more viscous with increasing temperature (Figs 3a & 4). The rheological model that describes the flow behaviour of the hydrated

suspension (i.e. without thermal ageing) is the Power Law. Thermal ageing introduced pseudoplastic flow behaviour, which is described by the Herschel & Bulkley model. The Power Law and Herschel & Bulkley models describe pseudoplastic fluids, as $n < 1$. Gel formation was spontaneous at temperatures $>149^\circ\text{C}$, which is an indication of the extensive delamination of hectorite particles that led to sharp increases in PV and AV. The gel was completely broken down when shear stress was applied.

Saponite suspensions presented inferior rheological performance to hectorite (Fig. 3b). Viscosity increased after thermal ageing up to 149°C and decreased at higher temperatures (Table 4), suggesting that the dispersions collapsed at high temperatures. The API standards determine the acceptable AV limit at 15 cP (i.e. 15 mPa·s; Temraz & Hassanien, 2016), so saponite suspensions at 100°C and 149°C comply with the API specifications, although the suspension concentration was 5% instead of 6.42%. At room temperature, saponite dispersion is described by the Bingham Plastic model. After thermal ageing, all suspensions could be described by the Herschel & Bulkley model (Table 4).

The stevensite suspensions were completely inert at temperatures $<176^\circ\text{C}$, with shear stress values being close to the detection limit of the viscometer (5 dyn cm^{-2}) for the suspensions aged at 25°C and 100°C (Figs 3c & 4). However, the suspensions did not show evidence of collapse. The formation of a suspension with high PV and AV and a YP at 230°C (Figs 3c & 4 & Table 4) was an unexpected result, which suggests possible delamination of stevensite particles and the formation of particle networks.

In the sepiolite suspensions, higher temperatures facilitated hydration of particles, leading to augmented rheological behaviour (Altun *et al.*, 2010). Indeed, the viscosity increased gradually with the temperature of ageing, although the viscosity of the suspensions after ageing up to 149°C is very low (Figs 3c & 4 & Table 4). Despite the profound increase of viscosity, sepiolite does not comply with API specifications because it formed thin suspensions that, however, did not collapse or aggregate. Sepiolite consists of fibrous crystals, whereas the smectites in bentonites form mostly flake/platelet-like crystals (Christidis, 2011). The latter introduce greater hydrodynamic drag and thus contribute to the formation of viscous suspensions. Sepiolite displays plastic flow behaviour at temperatures $>176^\circ\text{C}$ (Fig. 3c & Table 4).

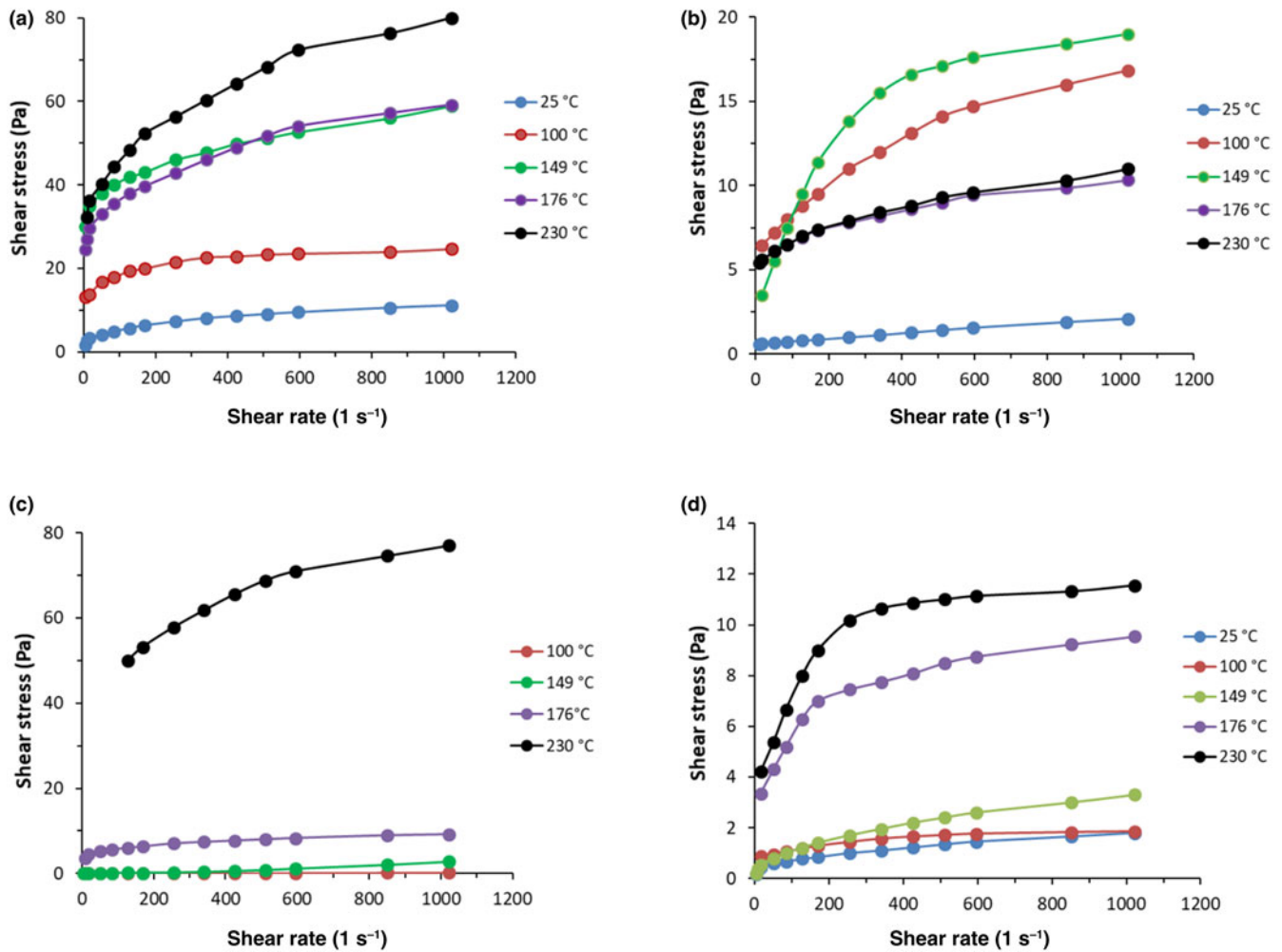


Figure 3. Rheograms of the clay suspensions aged at different temperatures. (a) hectorite; (b) saponite; (c) stevensite; (d) sepiolite.

Table 4 summarizes the YP values and YP/PV ratios of the suspensions, as well as the τ_0 , K and n values for the Herschel & Bulkley model corresponding to the yield stress, the consistency index and the flow-behaviour index of the suspension. These parameters were obtained both from the curve-fitting Herschel

& Bulkley model and from the logarithmic form of the Herschel & Bulkley equation, namely $\log(t - t_0) = \log K + n \log(\dot{\gamma})$. YP is affected by the particle interactions *via* van der Waals attractive forces (Vryzas *et al.*, 2016). The maximum acceptable value for YP is 18 lb 100 ft⁻² (~8.6 Pa) according to API 13A

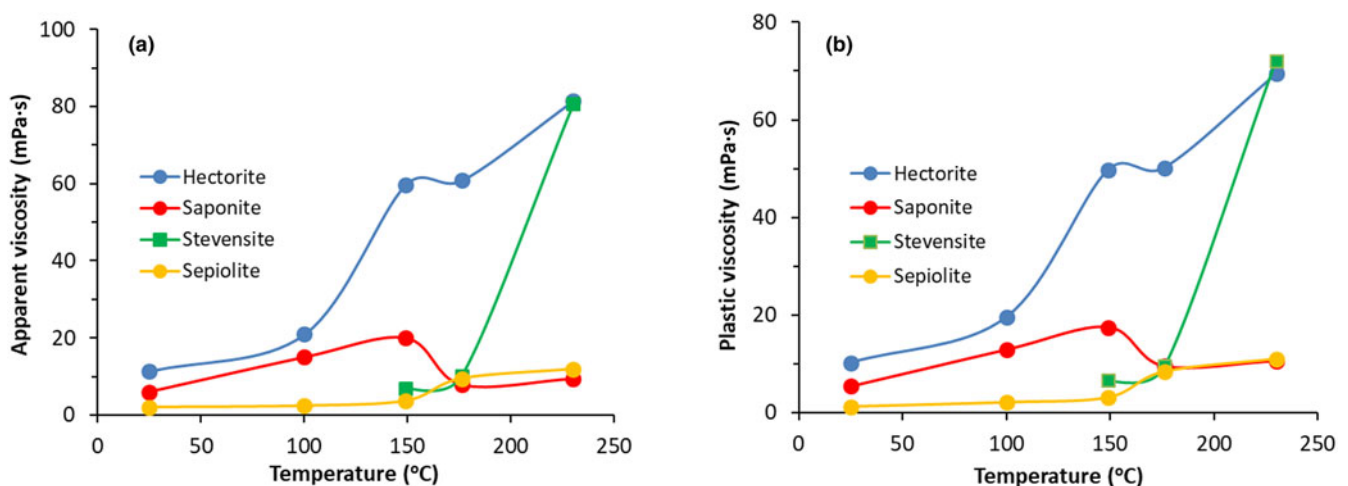


Figure 4. (a) AV and (b) PV of the suspensions as a function of temperature.

Table 4. PV, AV and YP of the suspensions ($PV = \Phi_{600} - \Phi_{300}$, $AV = \Phi_{600}/2$) determined according to API 13A specifications (API 13A, 2010).

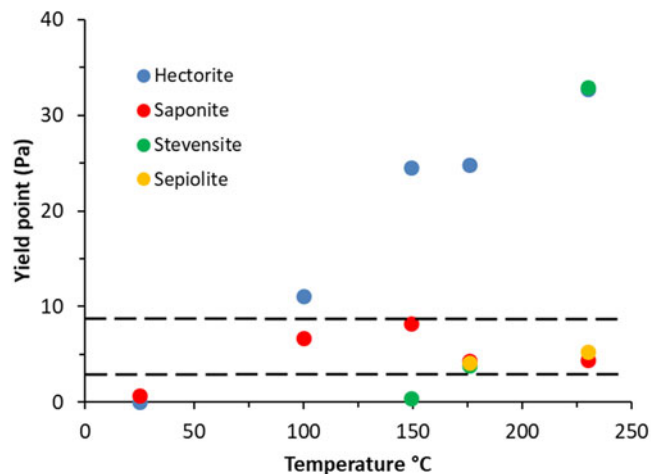
Sample	Rheological parameter	Temperature (°C)				
		25	100	149	176	230
Hectorite	PV (mPa-s)	10.3	19.6	49.8	50.2	69.5
	AV (mPa-s)	11.4	21.0	59.7	60.8	81.4
	YP (Pa)	–	11.1	24.5	24.8	32.7
	YP/PV	–	0.57	0.49	0.49	0.47
	Rheological model	–	H&B	H&B	H&B	H&B
	τ_0 (Pa)	–	10.5	28.6	24.1	31.3
	K (Pa·s ^{<i>n</i>})	–	2.48	2.02	1.46	1.36
	<i>n</i>	–	0.26	0.39	0.47	0.52
Saponite	PV (mPa-s)	5.5	12.9	17.5	9.6	10.6
	AV (mPa-s)	6.0	15.0	19.9	7.8	9.4
	YP (Pa)	0.7	6.7	8.2	4.3	4.4
	YP/PV	0.13	0.52	0.47	0.45	0.42
	Rheological model	BP	H&B	H&B	H&B	H&B
	τ_0 (Pa)	–	5.3	7.5	5.1	5.2
	K (Pa·s ^{<i>n</i>})	–	0.25	0.20	0.15	0.11
	<i>n</i>	–	0.56	0.60	0.51	0.57
Stevensite	PV (mPa-s)	–	–	3.3	9.5	72.1
	AV (mPa-s)	–	–	3.7	10.1	80.7
	YP (Pa)	–	–	0.4	3.8	32.9
	YP/PV	–	–	0.12	0.40	0.46
	Rheological model	–	–	H&B	H&B	H&B
	τ_0	–	–	0.3	2.2	30.1
	K (Pa·s ^{<i>n</i>})	–	–	0	0.97	3.34
	<i>n</i>	–	–	2.00	0.29	0.38
Sepiolite	PV (mPa-s)	1.2	2.1	3.1	8.4	11.1
	AV (mPa-s)	2.1	2.4	3.7	9.5	11.9
	YP (Pa)	–	–	–	4.1	5.3
	YP/PV	–	–	–	0.49	0.48
	Rheological model	–	–	–	H&B	H&B
	τ_0	–	–	–	3.2	3.8
	K (Pa·s ^{<i>n</i>})	–	–	–	0.44	0.81
	<i>n</i>	–	–	–	0.39	0.34

BP = Bingham Plastic model; H&B = Herschel & Bulkley model.

(2010). The YP/PV ratio expresses the pseudoplastic (shear thinning) behaviour of the suspension (Safi *et al.*, 2016), and the maximum acceptable value is 3 (API 13A, 2010). Both of the aforementioned limits apply to bentonite muds. Distinct limits for sepiolite dispersions are not available. The YP/PV ratios of all suspensions conform to the API specifications, although the solid content was 5% instead of 6.42%.

The YP during the experiments varies amongst the materials. In general, the YP of the suspensions increases with temperature, with a more profound effect occurring in the case of hectorite (Fig. 5). A similar trend was observed for dioctahedral Wyoming montmorillonite for ageing temperatures up to 80°C (Vryzas *et al.*, 2017). In fact, gel formation in hectorite suspensions was pronounced at temperatures >149°C, with the YP exceeding the maximum acceptable limit (i.e. ~8.6 Pa). The same applies to the stevensite suspension aged at 230°C. The remaining stevensite suspensions yielded low or undetectable YPs. Saponite and sepiolite muds exhibited low YPs and compliance with the API regulations (minimum YP of 1.5 Pa); thus, the YPs of these suspensions would not undermine their ability to transport fragmented rock during drilling operations.

The τ_0 , K and n parameters for the suspensions of the different Mg-clays at the various temperatures display certain trends (Table 4). In hectorite, the yield stress (τ_0) and flow-behaviour index (n) values increase with increasing ageing temperature, whereas the consistency index (K) shows the opposite trend. Similarly to hectorite, the K parameter of saponite decreases

**Figure 5.** YP of the examined suspensions after ageing at various temperatures. The dashed lines indicate the minimum and maximum YP values (in Pa) accepted by API 13A (2010).

gradually with increasing ageing temperature, whereas the τ_0 and n parameters are maximal after ageing at 149°C and decrease at greater ageing temperatures, similarly to what occurs in the viscosity of the suspensions (Fig. 5). The stevensite suspensions displayed gradual increases in τ_0 and K with increasing temperature, whereas n did not display a clear trend. Finally, sepiolite suspensions displayed gradual increases in τ_0 and K and a gradual decrease in n with increasing temperature (Table 4). In conclusion, all clay suspensions displayed an increase in τ_0 with increasing temperature, but sepiolite suspensions displayed the opposite trends with respect to the consistency index and flow-behaviour index trends compared with their hectorite and saponite counterparts, at least at high ageing temperatures for which sepiolite data are available. The trends for τ_0 , K and n observed for hectorite and saponite suspensions with increasing temperature are in agreement with those found in similar studies with suspensions of bentonites with dioctahedral smectites (Vryzas *et al.*, 2017). By contrast, the trends for τ_0 , K and n observed for stevensite suspensions are in general agreement with bentonite suspensions based on dioctahedral smectites, which contained laponite as an additive (Li *et al.*, 2022). However, laponite is not a pure phase but a mixture of 50% hectorite layers with 25% stevensite and 25% kerolite layers (Christidis *et al.*, 2018).

pH measurements

pH plays a key role in the performance of a multiphase fluid. Acidic conditions do not favour a bentonite-based suspension because the negative overall surface charge of the smectite particles is gradually neutralized and thus the electric double layer (EDL) is compressed (Park & Seo, 2011). This causes flocculation and sedimentation of particles. On the other hand, alkaline conditions contribute to the efficient dispersion of clay particles, as the net surface charge, which consists of the permanent and pH-dependent edge charges, is negative, and the EDLs expand and repel each other (Tombácz & Szekeres, 2004). The pH values obtained after ageing at various temperatures are listed in Table 5. The pH of suspensions increased with increasing ageing temperature in all of the trioctahedral clays (Fig. 6a & Table 5). The rheological parameters (PV, AV, YP) are improved at pH values >10 (Alaskari & Teymouri, 2007), which is also the case for most of

Table 5. pH measurements of the suspensions after 16 h of hydration (25°C) or thermal ageing.

Sample	25°C	100°C	149°C	176°C	230°
Hectorite	7.32	10.08	10.57	11.72	12.46
Stevensite	6.74	7.89	8.13	8.58	11.88
Saponite	7.56	7.61	9.37	9.15	9.52
Sepiolite	6.24	8.22	8.64	9.01	11.89

the suspensions prepared in this study. In particular, PV displays a well-expressed exponential increase with increasing pH, except for the sepiolite suspension aged at 230°C (Fig. 6b).

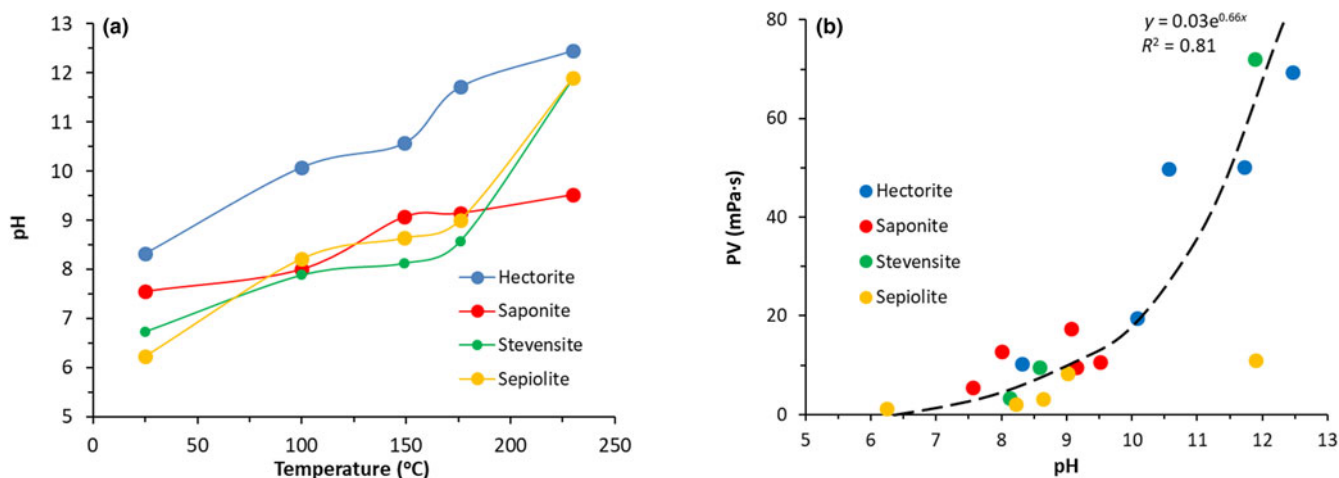
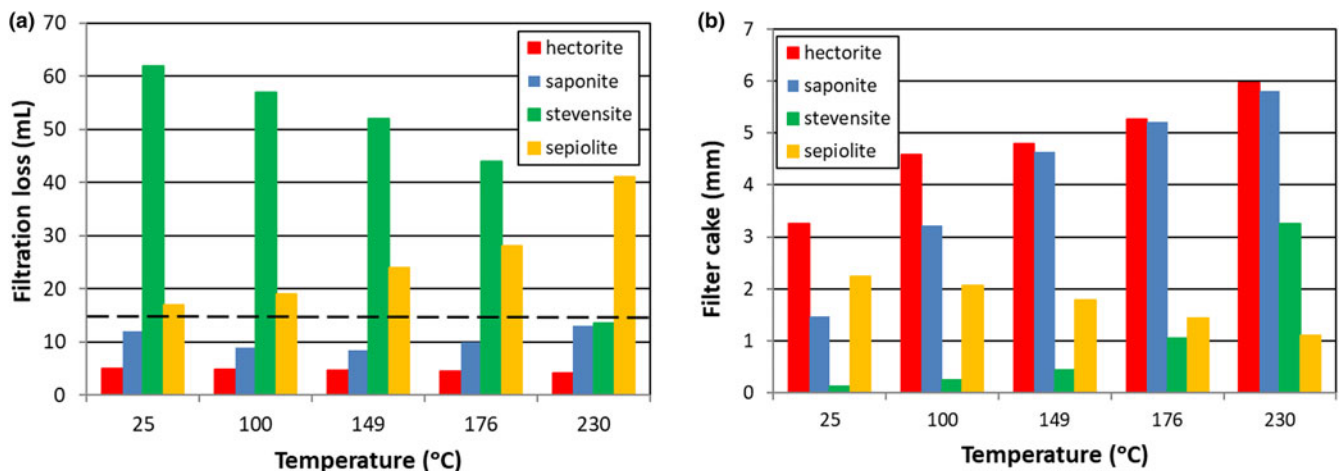
The hectorite suspensions are typical examples of the influence of alkaline pH on rheological properties, as the rheological behaviour was improved considerably compared to that of the remaining clay minerals (Fig. 6b). The same applies to the stevensite suspension at 230°C. Saponite suspensions became more alkaline with increasing temperature, and despite their collapse at 176°C (sharp decrease of the viscosity in Fig. 6b), the pH continued to increase. The pH of the sepiolite suspensions ranged between 6.2 and ~9.0, increasing sharply at 230°C (Fig. 6a), and the PV

increased sharply at 176°C and remained constant at greater temperatures (Fig. 6b).

Filtration loss and filter cake thickness

The stevensite and sepiolite suspensions did not comply with the maximum acceptable filtration loss of 15 mL according to the API 13A (2010) regulations for water-based drilling fluids (Fig. 7a). However, the hectorite and saponite muds did not produce large filtrate volumes. In fact, increasing temperature contributed to the reduction of filtration loss. Saponite suspensions collapsed at 176°C and 230°C, leading to extensive particle precipitation, which nevertheless did not significantly increase filtrate loss (Fig. 7a). The remaining filter cakes became thicker with increasing temperature for both saponite and hectorite suspensions. The thicker the filter cake, the more difficult it was for the fluid to penetrate it.

Stevensite suspensions expelled large volumes of fluid, far beyond the accepted limit. However, after a thermal ageing cycle at 230°C, the dispersion became viscous and the filtration loss complied with the API 13A specification, forming a thick filter cake (>3 mm). The sepiolite also displayed high filtration loss at all temperatures, indicating gel structures with open pores. In

**Figure 6.** (a) Evolution of the pH of the suspensions with temperature and (b) evolution of PV with pH.**Figure 7.** (a) Filtration loss of the suspensions and (b) thickness of the filter cakes after ageing at various temperatures. The dashed line in (a) indicates the maximum acceptable filtrate loss according to API 13A (2010).

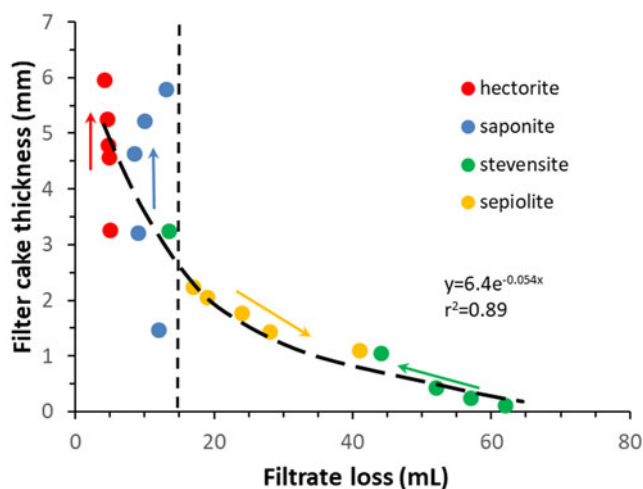


Figure 8. Filtrate loss vs filter cake thickness of the suspensions aged at various temperatures. The arrow for each clay mineral indicates the direction of increasing ageing temperature. The dashed line indicates the maximum acceptable filtrate loss according to API 13A (2010).

contrast to the smectite suspensions, the performance of sepiolite became poorer with increasing temperature. The filter cakes of the sepiolite suspensions were thin, acquiring a maximum thickness of 2.25 mm at a 25°C ageing temperature (Fig. 7b).

A well-defined overall negative exponential trend holds between the filtrate loss and thickness of the filter cakes (Fig. 8), indicating an association of high filter losses with thin filter cakes, as is to be expected. Maximum filter cake thickness/minimum filtrate loss was observed at greater ageing temperatures, with the sepiolite suspensions deviating from the overall trend. In general, a filtrate loss of <15 ml was observed in filter cakes thicker than ~3 mm, except for in the saponite suspension aged at 25°C (Fig. 8).

Chemical composition of the filtrates

Table 6 lists the concentrations of Na⁺ and Mg²⁺ cations of the filtrates. The Na⁺ and Mg²⁺ concentrations were used to assess the extent of cation exchange on bentonites after alkaline activation. In addition, the magnesium content was used to monitor possible decomposition of the smectite and sepiolite particles during thermal ageing.

The various bentonites display differing trends with respect to the Na content of the filtrates. The Na content of the hectorite filtrates increases with increasing temperature, reaching a plateau at >176°C, whereas the Na content in the saponite decreases slightly, and in the stevensite filtrates it decreases significantly, especially after ageing at 230°C. The high Na content of the stevensite

suspensions indicates that ageing up to 149°C does not facilitate Na-exchange, which begins at 176°C and is more effective at 230°C. The effective Na-exchange at 230°C is reflected in the improved rheological properties. However, the relatively low Na⁺ content of the hectorite suspensions indicates successful cation exchange during activation, which is in accordance with the superior rheological properties of the suspensions. Finally, the saponite filtrates also have relatively high Na contents, suggesting incomplete cation exchange.

Similarly, the Mg content of the filtrates varies amongst the various clay suspensions. The hectorite filtrates display rather constant and high Mg concentrations up to 176°C, which increases further after thermal ageing at 230°C, although the amount of Mg²⁺ remains essentially constant at ~0.6 meq throughout the whole ageing temperature range, because the filtrate volume decreases (Fig. 7a). Ion exchange (i.e. Na for Mg), although it might take place to some extent, is not considered the main driving force for the Mg²⁺ contents in the hectorite filtrates because of the rather high Mg/Na meq ratios (Table 6). By contrast, the saponite and sepiolite filtrates display low Mg contents. Finally, the stevensite filtrates have moderate Mg concentrations that increase after ageing at 176°C and especially at 230°C. However, the total amount of Mg in meq in the stevensite filtrates tends to decrease with increasing ageing temperature because the filtrate volume decreases considerably (Fig. 7a & Table 6). Similarly to the hectorite suspensions, ion exchange is not the main driving force of the Mg²⁺ content in stevensite because of the high Mg/Na meq ratios (Table 6). By contrast, the Na for Mg-exchange in saponite might be the dominant mechanism controlling the concentrations of these ions in the filtrates due to the rather high Na/Mg meq ratios (Table 6).

The Mg content displays a positive trend with the pH of the filtrates for the hectorite and the stevensite suspensions (Fig. 9), suggesting a contribution of dissolved Mg to the alkalinity of the suspensions. The saponite and sepiolite suspensions do not follow this trend due to their low Mg contents. The increase in Mg concentration in the hectorite and stevensite suspensions with temperature is in accordance with the increase in the pH of the filtrates with temperature (Fig. 6a & Table 5).

Discussion

Response of the trioctahedral clays to high-temperature ageing

The present study showed that the different trioctahedral clay minerals display different rheological properties and that the filtrate compositions can also vary significantly after thermal ageing. The Na⁺ and Mg²⁺ contents of the filtrates are controlled by ion exchange and the structural stability of the trioctahedral clay minerals. Considering the Mg content of the filtrates after thermal

Table 6. Concentrations of Na⁺ and Mg²⁺ cations (ppm) in the filtrates at various ageing temperatures. The values in parentheses are the amounts of Na⁺ and Mg²⁺ in meq.

Sample	Na ⁺					Mg ²⁺				
	25°C	100°C	149°C	176°C	230°C	25°C	100°C	149°C	176°C	230°C
Hectorite	183 (0.04)	254 (0.05)	365 (0.07)	504 (0.10)	532 (0.10)	1547 (0.64)	1426 (0.57)	1614 (0.63)	1479 (0.56)	1854 (0.65)
Saponite	1809 (0.94)	1723 (0.90)	1703 (0.89)	1706 (0.89)	1659 (0.87)	46 (0.05)	89 (0.07)	111 (0.08)	108 (0.09)	137 (0.15)
Stevensite	7044 (19.00)	7053 (17.50)	6988 (15.80)	5322 (10.20)	1078 (0.63)	587 (3.04)	594 (2.82)	612 (2.65)	898 (3.23)	2006 (2.26)
Sepiolite	-	-	-	-	-	35 (0.05)	45 (0.07)	49 (0.10)	61 (0.14)	66 (0.23)

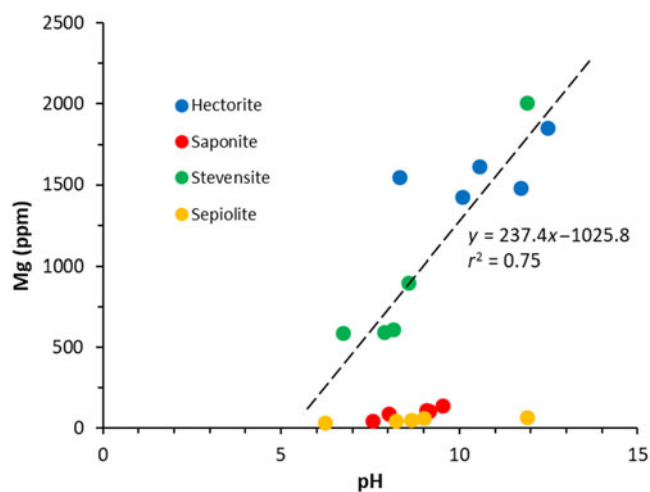


Figure 9. pH vs Mg content of the suspension filtrates after ageing at various temperatures.

ageing as a proxy for the stability of the clay minerals, when the Mg content exceeds the Na content, sepiolite displayed greater thermal stability than the trioctahedral smectites, and saponite had the greatest thermal stability amongst all of the trioctahedral smectites (Table 6). However, hectorite filtrates had high Mg^{2+} contents that tended to remain constant up to 176°C, increasing slightly after ageing at 230°C (Table 6). The high Mg^{2+} contents, even at ambient temperature, suggest that the Mg content of the filtrates might not result mainly from the dissolution of smectite but rather from the dissolution of other Mg-bearing phases, such as dolomite, or from the dissolution of soluble Mg salts. Indeed, the XRD results showed that dolomite dissolved after thermal ageing of the hectorite. Therefore, hectorite displayed very good thermal stability at high temperatures that is comparable to that of saponite.

The low Mg content of the saponite filtrates might be also attributed – at least partially – to Na-for-Mg exchange. In any case, saponite displayed inferior rheological properties at high temperatures compared to the other trioctahedral smectites, and its suspensions collapsed at temperatures >149°C (Fig. 5 & Table 4). By contrast, both hectorite and stevensite suspensions, with greater Mg contents, yielded viscous suspensions at high temperatures. The Na and Mg contents of the stevensite filtrates might also indicate limited Na-for-Mg exchange, as noted above. However, the existence of octahedral vacancies in the stevensite structure due to the lack of octahedral Mg suggests that Mg was not exchangeable and that the Mg^{2+} in the filtrates was probably due to modifications of the stevensite structure, except for the dissolution of dolomite. The appearance of a diffraction maximum at 10–11 Å (Fig. 1b), which might be attributed to kerolite layers, is in accordance with such a modification. This complex behaviour suggests that rheological properties at high temperatures might not be associated only with the stability of the crystal structure and particle morphology of the different trioctahedral clay minerals. Two additional parameters are considered further: the role of Na-exchange (Na-activation) and the intrinsic properties of clay mineral particles related to their crystal structure.

Na-exchange was relatively effective in hectorite, the filtrates of which showed low Na contents that slightly increased with increasing ageing temperature. This is also indicated in the d_{001}

of hectorite after thermal ageing (13–14 Å; Fig. 1b). The presence of Mg ions in the suspension due to dissolution of dolomite explains the incomplete Na-exchange in hectorite. A possible negative influence of temperature on Na-for-Ca/Mg exchange (e.g. Deist & Talibudeen, 1967) is not considered important because the exchange was not complete at room temperature in all filtrates, except for those of hectorite; instead, it was effective in stevensite at 230°C (Table 6). In addition, the saponite filtrates had high Na contents at all ageing temperatures, with a tendency to decrease slightly with increasing temperature, especially at 230°C, and low Mg contents. The lack of a particular trend in the Na content of filtrates with temperature suggests that Na-exchange might be controlled by the intrinsic properties of the individual smectites rather than temperature. The intrinsic properties considered in this study are layer charge and charge localization.

Layer charge affects ion exchange in both univalent and bivalent cations (Maes & Cremers, 1977a,b; Shainberg *et al.*, 1987). The selectivity for K over Ca or Na increases with increasing layer charge in natural smectites (Shainberg *et al.*, 1987) and in smectites with reduced layer charge (Maes & Cremers, 1977a, b). By contrast, in natural smectites, the layer charge does not affect Ca-for-Na exchange (Shainberg *et al.*, 1987). Layer charge seems to affect ion exchange by means of steric effects associated with swelling of the smectite layers (Verburg & Baveye, 1994; Laird *et al.*, 1995). However, the preference for a particular cation is associated more with partition of the cation between the aqueous solution and the smectite surface than the selectivity of the surface for a particular cation (Teppen & Miller, 2006; Rotenberg *et al.*, 2009). Yet, although stevensite has lower layer charge than hectorite and saponite, and therefore Na-exchange should have been facilitated, this was not observed in the present study (Table 6).

Charge localization and the source of charge are different in the various trioctahedral smectites. Hectorite and stevensite have octahedral layer charge, whereas saponite has tetrahedral layer charge. In addition, the source of charge in hectorite and saponite stems from substitutions within the octahedral sheet (Li for Mg) and the octahedral sheet (Al for Si), respectively, whereas the layer charge of stevensite is due to octahedral vacancies (Brigatti *et al.*, 2013). The surfaces of smectite with tetrahedral charge are more hydrophilic compared to their counterparts with octahedral charge due to the control of the tetrahedral Al on the maxima and minima of the potential curves on the surface of smectite, which affect the hydrophobicity of the surface (Bleam, 1990; Szczerba *et al.*, 2020).

Nevertheless, charge localization does not explain the behaviour of stevensite, which displayed enhanced Na-for-Ca exchange only after thermal ageing at 230°C. Indeed, although stevensite and hectorite bear octahedral charge, they displayed different responses in terms of Na-exchange at all temperatures except for 230°C. In both minerals, dissolution of dolomite released Mg^{2+} cations into the solution. The different response of stevensite to thermal ageing compared to hectorite is attributed to the particular nature of this mineral. Most stevensites are actually mixed-layer phases, consisting of a swelling phase (stevensite ss) and non-swelling kerolite (Eberl *et al.*, 1982; Jones & Weir 1983). Although the Moroccan stevensite used in this study does not show evidence of mixed layering (e.g. Christidis & Koutsopoulou, 2013), the small ratio of vacant octahedra, which contribute to the layer charge, to the occupied octahedra (~1:27; c.f. Rhouta *et al.*, 2008) suggests that the uncharged non-swelling kerolite domains (talc-like), which

have hydrophobic surfaces, promoted particle aggregation. At high temperatures, stevensite showed evidence of discrete kerolite-like layers (Fig. 1b). The appearance of discrete kerolitic domains suggests that the charged domains might have been preferentially dissolved, enhancing particle disaggregation through separation of the charged from the uncharged domains and therefore improving the rheological properties at high temperatures.

Finally, the possibility for crystallization of other phases during high-temperature ageing, such as analcime or albite (Güven, 1992), and its influence on the rheological properties were not considered in this study because such phases did not form during thermal ageing (Fig. 1b).

Use of trioctahedral clays in high-temperature drilling muds

Due to their high dehydroxylation temperatures, trioctahedral clay minerals have greater thermal stability than their dioctahedral counterparts. Therefore, they are possible candidates for the formulation of drilling muds that are employed in high-temperature wells, provided that, in the case of smectites, the interlayer cation is Na. All smectites used in this study were Na-activated, but only hectorite muds developed satisfactory rheological properties, with the behaviour of the remaining clays being unpredictable. The inferior rheological properties of saponite might be attributed to the incomplete Na-exchange because they are expected to display a greater tendency for adsorbing hydrated cations and swelling, thus facilitating ion exchange, provided that they do not collapse. Yet, after ageing, the d_{001} of saponite was centred at 13–14 Å, and a minor shoulder indicative of Na layers appeared at ~12.8 Å (Fig. 1b). The incomplete Na-exchange in the saponite interlayer with respect to hectorite might reflect the influence of charge localization on the exchange. The saponite is dominated by a tetrahedral charge. Hence, it could be considered that this tetrahedral charge might hinder the Na-for-Ca exchange. Nevertheless, the concentration of Na_2CO_3 used to activate the clay was 6%, suggesting that only a fraction of the added Na was not exchanged. Therefore, the incomplete Na-exchange cannot explain the inferior rheological properties of saponite.

Although charge localization does not account for the observed incomplete Na-exchange in saponite, it might be considered for the interpretation of the rheological properties. Dioctahedral smectites with a tetrahedral charge have inferior rheological properties compared to their counterparts with an octahedral charge of similar magnitude located in octahedral sites (Christidis *et al.*, 2006) because the tetrahedral charge will control the maxima of the potential curves on the surface of smectite (Bleam, 1990), which will lead to the aggregation of layers and thus to the suppression of the diffuse double layers. A similar behaviour is suggested for the trioctahedral smectites. Therefore, saponites are not expected to develop satisfactory rheological behaviour at any temperature, although the tetrahedral charge seems to provide greater thermal stability against dissolution in the temperature range considered in this study. Nevertheless, the rheological behaviour might be improved with the addition of suitable additives, but this is beyond the scope of this work.

Stevensite displayed differing rheological behaviour from hectorite, although they both have octahedral charge and the layer charge of stevensite is lower than that of hectorite (Christidis & Eberl, 2003; Rhouta *et al.*, 2008). The small ratio of vacant octahedra, which are the source of the layer charge, to the occupied octahedra (~1:27; c.f. Rhouta *et al.*, 2008) suggests that the uncharged non-swelling kerolite domains hinder Na-exchange.

Inasmuch as the uncharged kerolite layers are expected to be hydrophobic, similarly to talc layers, they impede Na-exchange in the charged layers, causing limited swelling and thus inferior rheological properties. Dolomite dissolution hindered Na-exchange further. The preferential dissolution of the vacant octahedra compared to their occupied counterparts during high-temperature ageing facilitated particle separation and thus Na-exchange, thereby promoting Na-activation of the stevensite. Therefore, stevensite drilling fluids seem to be promising for high-temperature applications.

Hectorite suspensions presented superior rheological performance to all of the other examined clay minerals, even though the content of hectorite in the sample was <50% and dolomite dissolution hindered Na-exchange. Thermal ageing increased the PV and AV of hectorite suspensions, which demonstrated plastic flow behaviour. The extensive gel formation of hectorite suspensions led to the YP being reached, which is associated with the hydration of clay particles and the electrostatic interactions amongst them. The YP is a function of the number and strength of particle–particle bonds (van Olphen, 1964; Neaman & Singer, 2000a). In addition, hectorite displayed very good thermal stability over the whole temperature range used in this study. Therefore, hectorite is an excellent material for the formulation of drilling fluids for high-temperature applications.

The rheological properties of sepiolite were inferior to those of its bentonite counterparts. The rheological performance of fibrous clays is connected to their fibre length, CEC (which is low) and specific surface area (Simonton *et al.*, 1988; Neaman & Singer, 2000b). The silanol groups at the external sepiolite surfaces bind the fibrous sepiolite crystals, forming networks and thus affecting the AV and YP of sepiolite suspensions (Simonton *et al.*, 1988). However, the sepiolite did not develop suspensions with acceptable rheological behaviour, and a similar rheological behaviour was observed in a preliminary study of a Spanish sepiolite (data not shown). Nevertheless, the thermal stability of sepiolite at high temperatures indicates that it might be rendered suitable for high-temperature drilling applications after the addition of suitable additives. More information regarding the structural characteristics (e.g. specific surface area, fibre length, etc.) and use of additives in this context is necessary to support this suggestion.

Conclusions

This study examined the influence of thermal ageing (up to 230°C) on 5% suspensions of Mg-bentonites containing trioctahedral smectites (hectorite, stevensite and saponite) after activation with Na_2CO_3 and a sepiolite clay, and it yielded the following conclusions.

In general, thermal ageing did not affect the thermal stability of the clays. Except for stevensite clay at 230°C, the clay minerals displayed minimal dissolution after thermal ageing. Hectorite and saponite displayed the best thermal stability at all temperatures, whereas stevensite crystals displayed dissolution features and partial conversion to kerolite after thermal ageing at 230°C. Thermal stability (recorded as resistance to dissolution), the response to Na-activation and the rheological properties of the clays are directly associated with the crystal structure: namely, layer charge and charge localization, the particle shape of the clay minerals present and the presence of Mg-accessory minerals that might dissolve during thermal ageing, such as dolomite.

Based on the rheological properties, the sepiolite clay is considered unsuitable for drilling fluids at high temperatures. The

rheological properties were almost identical and inferior to bentonites, presenting a subtle, plastic flow behaviour at higher temperatures. Moreover, the filtrate loss volume exceeded 15 mL. In addition, the saponite clay is not recommended for drilling fluid applications as it collapses at greater temperatures. Moreover, it did not present acceptable YP and viscosity, and hence its lubricating, insulating and carrying performances do not meet API 13A specifications. Nevertheless, the sepiolite and saponite clay suspensions might meet API 13A specifications if the concentration of solids is raised to 6.42%.

The activation of the cation-exchange mechanism of stevensite clay at high temperatures makes it a suitable additive for drilling fluids in high-temperature operations such as high-enthalpy geothermal fields or deep oil well drilling. The intense gel formation leads to high YP values, which might cause malfunctions in the mud pumps. Consequently, the utilization of stevensite clays in drilling fluid applications is recommended, along with other viscosity- and gel formation-regulating agents.

The hectorite clay displayed excellent rheological properties that did not deteriorate with increasing temperature, although the hectorite content was low. Therefore, this hectorite clay is recommended for a wide range of drilling purposes. However, its concentration should remain low due to the development of viscous fluids with considerable amounts of gel, which might prove stressful to the pumping equipment.

Acknowledgements. This paper is a result of the diploma thesis of N. Athanasakis (mineral resources engineering MSc), carried out at the Mineral Resources Engineering Department, Technical University of Crete. Professor Dr G.E. Christidis was the supervisor and editor of this paper and Professor Dr D. Marinakis planned the rheological experiments.

Conflicts of interest. The authors declare none.

References

- Abdo J., Al-Sharji H. & Hassan E. (2016) Effects of nano-sepiolite on rheological properties and filtration loss of water-based drilling fluids. *Surface and Interface Analysis*, **48**, 522–526.
- Alaskari M.K.G. & Teymoori R.N. (2007) Effects of salinity, pH and temperature on CMC polymer and XC polymer performance. *International Journal of Engineering*, **20**, 283–290.
- Alderman N.J., Gavignet A.A., Guillot D. & Maitland G.C. (1988) High temperature, high pressure rheology of oil based muds. Presented at: *SPE 18035 Annual Technical Conference and Exhibition of the Society of Petroleum Engineers*, Houston, TX, USA, 2–5 October.
- Al-Malki N., Pourafshary P., Al-Hadrami H. & Abdo J. (2016) Controlling bentonite-based drilling mud properties using sepiolite nanoparticles. *Petroleum Exploration and Development*, **43**, 717–723.
- Altun G., Osgouei A.E. & Serpen U. (2010) Controlling rheological and fluid loss properties of sepiolite based muds under elevated temperatures. Presented at: *World Geothermal Congress 2010*. Bali, Indonesia, 25–29 April.
- Alvarez A. (1984) Sepiolite: properties and uses. Pp. 253–287 in: *Palygorskite–Sepiolite: Occurrences, Properties and Uses* (A. Singer & E. Galan, editors). Elsevier, Amsterdam, The Netherlands.
- API 13A (2010) *Specification for Drilling Fluids – Specification and Testing*. American Petroleum Institute, Washington, DC, USA, 128 pp.
- Bageri B.S., Gamal H., Elkhatatny S. & Patil S. (2021) Effect of different weighting agents on drilling fluids and filter cake properties in sandstone formations. *ACS Omega*, **6**, 16176–16186.
- Bavoh C.B., Adam J.M. & Lal B. (2022) Specific heat capacity of xanthan gum/PAC polymer-based drilling fluids: an experimental and correlation study. *Materials Today: Proceedings*, **57**, 1002–1007.
- Benhammou A., Tanouti B., Nibou L., Yaacoubi A. & Bonnet J.P. (2009) Mineralogical and physicochemical investigation of Mg-smectite from Jbel Ghassoul, Morocco. *Clays and Clay Minerals*, **57**, 264–270.
- Bergaya F. & Vayer M. (1997) CEC of clays: measurement by adsorption of a copper ethylene–diamine complex. *Applied Clay Science*, **12**, 275–280.
- Bleam W.F. (1990) The nature of cation-substitution sites in phyllosilicates. *Clays and Clay Minerals*, **38**, 527–536.
- Brandenburg U. & Lagaly G. (1988) Rheological properties of sodium montmorillonite dispersions. *Applied Clay Science*, **3**, 263–279.
- Brigatti M.F., Galan E. & Theng B.K.G. (2013) Structure and mineralogy of clay minerals. Pp. 21–81 in: *Handbook of Clay Science* (F. Bergaya, B.H.K. Theng & G. Lagaly, editors). Elsevier, Amsterdam, The Netherlands.
- Brindley G.W. (1984) Order–disorder in clay mineral structures. Pp. 125–195 in: *Crystal Structures of Clay Minerals and Their X-ray Identification* (G.W. Brindley & G. Brown, editors). Mineralogical Society of Great Britain & Ireland, London, UK.
- Briscoe B.J., Luckham P.F. & Ren S.R. (1994) The properties of drilling muds at high pressures and high temperatures. *Philosophical Transactions of the Royal Society of London. Series A: Physical and Engineering Sciences*, **348**, 179–207.
- Chemeda Y.C., Christidis G.E., Tauhid Khan N.M., Koutsopoulou E., Hatzistamou V. & Kelessidis V.C. (2014) Rheological properties of palygorskite–bentonite and sepiolite–bentonite mixed clay suspensions. *Applied Clay Science*, **90**, 165–174.
- Cheremisinoff N.P. (1986) *Encyclopedia of Fluid Mechanics*. Gulf Publishing, Houston, TX, USA, 570 pp.
- Christidis G.E. (1998) Physical and chemical properties of some bentonite deposits of Kimolos Islands, Greece. *Applied Clay Science*, **13**, 79–98.
- Christidis G.E. (2011) Assessment of industrial clays. Pp. 425–449 in: *Handbook of Clay Science* (F. Bergaya, B.H.K. Theng & G. Lagaly, editors). Elsevier, Amsterdam, The Netherlands.
- Christidis G.E., & Eberl D.D. (2003) Determination of layer charge of smectites. *Clays and Clay Minerals*, **51**, 644–655.
- Christidis G.E., & Koutsopoulou E. (2013) A simple approach to the identification of trioctahedral smectites by X-ray diffraction. *Clay Minerals*, **48**, 687–696.
- Christidis G.E. & Mitsis J. (2006) A new Ni-rich stevensite from the ophiolite complex of Othrys, central Greece. *Clays and Clay Minerals*, **54**, 653–666.
- Christidis G., & Scott P. W. (1996) Physical and chemical properties of bentonite deposits of Milos Island, Greece. *Applied Earth Science: Transactions of the Institutions of Mining and Metallurgy: Section B*, **105**, B165–B174.
- Christidis G.E., Aldana C., Chryssikos G.D., Gionis V., Kalo H., Stöter M. & Robert J.L. (2018) The nature of laponite: pure hectorite or a mixture of different trioctahedral phases? *Minerals*, **8**, 314.
- Christidis G.E., Blum A.E. & Eberl D.D. (2006) Influence of layer charge and charge distribution of smectites on the flow behaviour and swelling of bentonites. *Applied Clay Science*, **34**, 125–138.
- Deist J. & Talibudeen O. (1967) Ion exchange in soils from the ion pairs K–Ca, K–Rb, and K–Na 1. *Journal of Soil Science*, **18**, 125–137.
- Eberl D.D., Jones B.F., & Khoury H.N. (1982) Mixed layer kerolite/stevensite from the Amargosa Desert. *Nevada: Clays and Clay Minerals*, **30**, 321–326.
- Echt T. & Plank J. (2019) An improved test protocol for high temperature carrying capacity of drilling fluids exemplified on a sepiolite mud. *Journal of Natural Gas Science and Engineering*, **70**, 102964.
- Gamal H., Elkhatatny S., Basfar S. & Al-Majed A. (2019) Effect of pH on rheological and filtration properties of water-based drilling fluid based on bentonite. *Sustainability*, **11**, 6714.
- Gautam S., Guria C., Rajak D.K. & Pathak A.K. (2018) Functionalization of fly ash for the substitution of bentonite in drilling fluid. *Journal of Petroleum Science and Engineering*, **166**, 63–72.
- Gerogiorgis D.I., Clark C., Vryzas Z. & Kelessidis V.C. (2015) Development and parameter estimation for a multivariate Herschel–Bulkley rheological model of a nanoparticle-based smart drilling fluid. Pp. 2405–2410 in: *Computer Aided Chemical Engineering* (K.V. Gernaey, J.K. Huusom & R. Gani, editors). Elsevier, Amsterdam, The Netherlands.
- Grim R.E. (1962) *Applied Clay Mineralogy*. McGraw-Hill, New York, NY, USA, 180 pp.

- Grim R.E. (1968) *Clay Mineralogy*, 2nd edition. McGraw-Hill, New York, NY, USA, 596 pp.
- Guggenheim S. & Koster van Groos A.F. (2001) Baseline studies of The Clay Minerals Society Source Clays: thermal analysis. *Clays and Clay Minerals*, **49**, 433–443.
- Güven N. (1992) Rheological aspects of aqueous smectite suspensions. Pp. 81–125 in: *Clay–Water Interface and Its Rheological Implications* (N. Güven & R.M. Pollastro, editors). The Clay Minerals Society, Aurora, CO, USA.
- Güven N., Carney L.L. & Ridpath B.E. (1987) *Evaluation of Geothermal Drilling Fluids Using a Commercial Bentonite and a Bentonite/Saponite Mixture*. Technical report. US Department of Energy Office of Scientific and Technical Information, Oak Ridge, TN, USA, 114 pp.
- Güven N., Panfil D.J. & Carney L.L. (1988) Comparative rheology of water-based drilling fluids with various clays. Presented at: *International Meeting of Petroleum Engineering, Society on Petroleum Engineering*, Tianjin, China, 1–4 November.
- Hiller K.H. (1963) Rheological measurements of clay suspensions at high temperatures and pressures. *Journal of Petroleum Technology*, **17**, 779–789.
- İşçi E. & Turutoğlu S.İ. (2011) Stabilization of the mixture of bentonite and sepiolite as a water based drilling fluid. *Journal of Petroleum Science and Engineering*, **76**, 1–5.
- Johnston C.T. & Tombácz E. (2002) Surface chemistry of soil minerals. Pp. 33–67 in: *Soil Mineralogy with Environmental Applications* (J.B. Dixon & D.G. Schulze, editors). SSSA, Madison, WI, USA.
- Jones B.F., & Weir A.H. (1983) Clay minerals of Lake Albert, an alkaline, saline lake. *Clays and Clay Minerals*, **31**, 161–172.
- Kelessidis V.C. & Maglione R. (2008) Yield stress of water–bentonite dispersions. *Colloids and Surfaces A: Physicochemical and Engineering Aspects*, **318**, 217–226.
- Kelessidis V.C., Christidis G., Makri P., Hadjistamou V., Tsamantaki C., Mihalakis A. *et al.* (2007a) Gelation of water–bentonite suspensions at high temperatures and rheological control with lignite addition. *Applied Clay Science*, **36**, 221–231.
- Kelessidis V.C., Tsamantaki C., Pasadakis N., Repouskou E. & Hamilaki E. (2006) Permeability, porosity and surface characteristics of filter cakes from water–bentonite suspensions. *WIT Transactions on Engineering Sciences*, **56**, 173–182.
- Kelessidis V.C., Tsamantaki C. & Dalamarinis P. (2007b) Effect of pH and electrolyte on the rheology of aqueous Wyoming bentonite dispersions. *Applied Clay Science*, **38**, 86–96.
- Kelessidis V.C., Tsamantaki C., Michalakis A., Christidis G.E., Makri P., Papanicolaou K. & Foscolos A. (2007c) Greek lignites as additives for controlling filtration properties of water–bentonite suspensions at high temperatures. *Fuel*, **86**, 1112–1121.
- Lagaly G. (1989) Principles of flow of kaolin and bentonite dispersions. *Applied Clay Science*, **4**, 105–123.
- Laird D.A., Shang C., & Thomson M.L. (1995) Hysteresis in crystalline swelling of smectites. *Journal of Colloid and Interface Science*, **171**, 240–245.
- Li X.-L., Guan-Cheng Jiang G.G., Xu Y., Deng Z.Q. & Wang K. (2022) A new environmentally friendly water-based drilling fluids with laponite nanoparticles and polysaccharide/polypeptide derivatives. *Petroleum Science*, **19**, 2959–2968.
- Madejová J., Gates W.P. & Petit S. (2017) IR spectra of clay minerals. Pp. 107–149 in: *Infrared and Raman Spectroscopies of Clay Minerals* (W.P. Gates, J.T. Kloprogge, J. Madejová & F. Bergaya, editors). Elsevier, Amsterdam, The Netherlands.
- Maes A., & Cremers A. (1977a) Charge density effects in ion exchange. Part 1. – Heterovalent exchange equilibria. *Journal of the Chemical Society*, **73**, 1807–1814.
- Maes A., & Cremers A. (1977b) Charge density effects in ion exchange. Part 2. – Homovalent exchange equilibria. *Journal of the Chemical Society*, **74**, 1234–1241.
- McDonald M., Barr K., Dubberley S.R. & Wadsworth G. (2007) Use of silicate-based drilling fluids to mitigate metal corrosion. Presented at: *International Symposium on Oilfield Chemistry*. Houston, TX, USA, 28 February.
- McKee A. & Geehan T. (1989) Drilling mud: monitoring it and managing it. *Oilfield Review*, **1**, 41–52.
- Meunier A. (2005) *Clays*. Springer, Berlin, Germany, 307 pp.
- Miles W.J. (2011) Amargosa sepiolite and saponite: geology, mineralogy, and markets. Pp. 265–277 in: *Developments in Palygorskite–Sepiolite Research*. A *New Outlook on These Nanomaterials* (E. Galan & A. Singer, editors). Elsevier, Amsterdam, The Netherlands.
- Mohammed A.S. (2017) Effect of temperature on the rheological properties with shear stress limit of iron oxide nanoparticle modified bentonite drilling muds. *Egyptian Journal of Petroleum*, **26**, 791–802.
- Neaman A. & Singer A. (2000a) Rheological properties of aqueous suspensions of palygorskite. *Soil Science Society of America Journal*, **64**, 427–436.
- Neaman A. & Singer A. (2000b) Rheology of mixed palygorskite–montmorillonite suspensions. *Clays and Clay Minerals*, **48**, 713–715.
- Newman A.C.D. & Brown G. (1987) The chemical constitution of clays. Pp. 1–128 in: *The Chemistry of Clays and Clay Minerals* (A.C.D. Newman, editor). Mineralogical Society of London, London, UK.
- Odom I.E. (1984) Smectite clay minerals: properties and uses. *Philosophical Transactions of the Royal Society of London. Series A, Mathematical and Physical Sciences*, **311**, 391–409.
- Olphen H.V. (1964) Internal mutual flocculation in clay suspension. *Journal of Colloid Science*, **19**, 313–322.
- Olphen H.V. (1977) *Introduction to Clay Colloid Chemistry*, 2nd edition. Wiley and Sons, New York, NY, USA.
- Oort E.V., Hoxha B.B., Yang L. & Hale A. (2016) Automated particle size analysis using advanced analyzers. Presented at: *The IADC/SPE Drilling Conference*, Fort Worth, TX, USA, 1–3 March.
- Park S.J. & Seo M.K. (2011) Intermolecular force. *Interface Science and Technology*, **18**, 1–57.
- Rhouta B., Kaddami H., Elbarqy J., Amjoud M., Daoudi L. Maury F. *et al.* (2008) Elucidating the crystal-chemistry of Jbel Rhassoul stevensite (Morocco) by advanced analytical techniques. *Clay Minerals*, **43**, 393–404.
- Rotenberg B., Morel J.-P., Marry V., Turq P., & Morel-Desrosiers N. (2009) On the driving force of cation exchange in clays: insights from combined microcalorimetry experiments and molecular simulation. *Geochimica et Cosmochimica Acta*, **73**, 4034–4044.
- Safi B., Zarouri S., Chabane-Chauache R., Saidi M. & Benmounah A. (2016) Physico-chemical and rheological characterization of water-based mud in the presence of polymers. *Journal of Petroleum Exploration and Production Technology*, **6**, 185–190.
- Sainz-Diaz C.I., Hernandez-Laguna A. & Dove M.T. (2001) Theoretical modelling of *cis*-vacant and *trans*-vacant configurations in the octahedral sheet of illites and smectites. *Physics and Chemistry of Minerals*, **28**, 322–331.
- Santoyo E., Santoyo-Gutierrez S., García A., Espinosa G. & Moya S.L. (2001) Rheological property measurement of drilling fluids used in geothermal wells. *Applied Thermal Engineering*, **21**, 283–302.
- Shainberg I., Alperovich N.I. & Keren R. (1987) Charge density and Na–K–Ca exchange on smectites. *Clays and Clay Minerals*, **35**, 68–73.
- Simonton T.C., Komarneni S. & Roy R. (1988) Gelling properties of sepiolite versus montmorillonite. *Applied Clay Science*, **3**, 165–176.
- Szczerba M., Kalinichev A.G., & Kowalika M. (2020) Intrinsic hydrophobicity of smectite basal surfaces quantitatively probed by molecular dynamics simulations. *Applied Clay Science*, **188**, 105497.
- Temraz M.G. & Hassanien I. (2016) Mineralogy and rheological properties of some Egyptian bentonite for drilling fluids. *Journal of Natural Gas Science and Engineering*, **31**, 791–799.
- Teppen B.J., & Miller D.M. (2006) Hydration energy determines isoivalent cation exchange selectivity by clay minerals. *Soil Science Society of America Journal*, **70**, 31–40.
- Tombácz E. & Szekeres M. (2004) Colloidal behavior of aqueous montmorillonite suspensions: the specific role of pH in the presence of indifferent electrolytes. *Applied Clay Science*, **27**, 75–94.
- Tombácz E., Ábrahám I., Gilde M. & Szántó F. (1990) The pH-dependent colloidal stability of aqueous montmorillonite suspensions. *Colloids and Surfaces*, **49**, 71–78.
- Verburg K., & Baveye P. (1994) Hysteresis in the binary exchange of cations on 2:1 clay minerals: a critical review. *Clays and Clay Minerals*, **42**, 207–220.
- Vryzas Z. & Kelessidis V.C. (2017) Nano-based drilling fluids: a review. *Energies*, **10**, 540.
- Vryzas Z., Wubulikasimu Y., Gerogiorgis D. & Kelessidis V.C. (2016) Understanding the temperature effect on the rheology of water–bentonite suspensions. *Annual Transactions of the Nordic Rheological Society*, **24**, 199–208.

- Vryzas Z., Kelessidis V.C., Nalbantian L., Zaspalis V., Gerogiorgis D.I. & Wubulikasimu Y. (2017) Effect of temperature on the rheological properties of neat aqueous Wyoming sodium bentonite dispersions. *Applied Clay Science*, **136**, 26–36.
- Wolters F. & Emmerich K. (2007) Thermal reactions of smectites – relation of dehydroxylation temperature to octahedral structure. *Thermochimica Acta*, **462**, 80–88.
- Xiong Z.Q., Fu F. & Li X.D. (2019a) Experimental investigation on laponite as ultra high-temperature viscosifier of water-based drilling fluids. *SN Applied Sciences*, **1**, 1374.
- Xiong Z.Q., Li X.D., Fu F. & Yan-Ning L. (2019b) Performance evaluation of laponite as a mud-making material for drilling fluids. *Petroleum Science*, **16**, 890–900.
- Zhang J.R., Xu M.D., Christidis G.E. & Zhou C.H. (2020) Clay minerals in drilling fluids: functions and challenges. *Clay Minerals*, **55**, 1–11.
- Zhuang G., Zhang Z., Peng S., Gao J. & Jaber M. (2018) Enhancing the rheological properties and thermal stability of oil-based drilling fluids by synergistic use of organo-montmorillonite and organo-sepiolite. *Applied Clay Science*, **161**, 505–512.